1. INTRODUCTION

Sunspots are dark because normal convection is suppressed by a strong magnetic field, which allows only weaker time-dependent motion. Attempts to explain this effect led to the systematic study of magnetoconvection, revealing a complicated pattern of oscillatory and stationary solutions. Indeed, the subject has now outgrown its original astrophysical motivation and can be investigated as an example of competition between stabilizing and destabilizing mechanisms, which gives rise to a rich variety of dynamical behaviour (see Hughes and Proctor, 1988; Weiss, 1991; Proctor, 1992 and references therein).

In the astrophysically relevant regime, where the field is strong and the magnetic diffusivity is much smaller than the (radiative) thermal diffusivity, there are two primary bifurcations from the trivial static solution: in idealized models, convection sets in at an oscillatory (Hopf) bifurcation, which is followed by a stationary (pitchfork) bifurcation as the rate of heating (measured by a Rayleigh number R) is increased. By varying a second parameter, such as the aspect ratio, it is possible to locate a bifurcation of codimension two, where the Hopf and pitchfork bifurcations coincide. Such multiple bifurcations are important, for nonlinear behaviour in their neighbourhoods can be investigated analytically; moreover, they act as organizing centres for a large region of parameter space. In cases that have previously been discussed, the branch of nonlinear periodic solutions terminates on the branch of steady solutions that emerges from the primary pitchfork bifurcation, either in a secondary Hopf bifurcation or in a heteroclinic bifurcation (Proctor and Weiss, 1982). Such oscillations only exist when the pitchfork is preceded by a Hopf bifurcation as R is increased.

Nonlinear behaviour can also be explored by solving the appropriate partial differential equations (PDEs) numerically in some idealized configuration. Numerical experiments on two-dimensional compressible magnetoconvection revealed a feature that had not been anticipated. As the aspect ratio was decreased beyond the codimension-two point, nonlinear oscillations persisted, although the primary Hopf bifurcation had disappeared. Closer investigation showed that after being created in the pitchfork bifurcation, the steady solutions lost stability in a secondary Hopf bifurcation, so giving rise to the prominent oscillatory solutions (Weiss *et al.*, 1990). This scenario is not a consequence of compressibility and could also be found in Boussinesq magnetoconvection.

This particular example illustrates an important effect: a system with a propensity to oscillate may exhibit periodic behaviour over a wide parameter range although linear theory provides no indication of a primary Hopf bifurcation from the trivial solution as a single stability parameter is varied. The purpose of this paper is to analyse the mechanism that leads to such behaviour in double convection. We shall show how the results of numerical experiments on nonlinear magnetoconvection can be related to the properties of low-order systems of ordinary differential equations (ODEs) that accurately model the full PDEs. Indeed, the appropriate normal form equation (Arnol'd, 1983; Guckenheimer and Holmes, 1983) shows that if the primary Hopf bifurcation is subcritical on one side of the codimension-two bifurcation then, on the other side, there must be a branch of stable oscillatory solutions emerging from a supercritical secondary Hopf bifurcation. Thus this problem provides a fine demonstration of the power of nonlinear dynamics in interpreting numerical experiments.

We shall confine our attention to two-dimensional compressible magnetoconvection in a strongly stratified layer (as a model of behaviour in the umbra of a sunspot). The governing PDEs are given in the next section, where linear theory is used to calculate the critical value, λ_c, of the aspect ratio λ at the codimension-two bifurcation. Previous computations, showing the appearance of a secondary Hopf bifurcation, (Weiss *et al.*, 1990) are also summarized. In Section 3 we present new results, obtained by integrating the PDEs numerically, for values of λ on either side of λ_c. These numerical experiments show that the secondary Hopf bifurcation (for $\lambda < \lambda_c$) is associated with a subcritical primary Hopf bifurcation (for $\lambda > \lambda_c$). This behaviour is related to a second-order system of ODEs (the amplitude equations) in Section 4. We show first that the normal form equation for a Takens–Bogdanov bifurcation with Z_2 symmetry predicts behaviour similar to that found for the

PDEs; then we explore the consequences of including a fifth-order correction in the amplitude equations. In Section 5 we return to the PDEs and confirm that the oscillatory branches terminate in a final Hopf bifurcation from the branch of steady solutions, as predicted by the corrected amplitude equations. The bifurcation structure is, however, complicated by the appearance of stable travelling wave as well as standing wave solutions (cf. Hurlburt *et al.*, 1989). The role of travelling waves is clarified by reference to appropriately modified amplitude equations in Section 6. The implications of our results are summarized in the final section.

2. THE SECONDARY HOPF BIFURCATION IN COMPRESSIBLE MAGNETOCONVECTION

We shall consider an idealized model of two-dimensional fully compressible convection in a perfect monatomic gas occupying the region $\{0 \le x \le \lambda; z_0 \le z \le z_0 + 1\}$, with z increasing downwards, in the presence of an imposed vertical magnetic field. Then there is a static solution corresponding to a polytrope of index m, with a density contrast $\chi = [(z_0 + 1)/z_0]^m$. The velocity $\mathbf{u} = (u, 0, w)$, magnetic field $\mathbf{B} = (B_x, 0, B_z)$, density ρ, pressure P and temperature T satisfy the nondimensional equations

$$\frac{\partial}{\partial t}(\rho \mathbf{u}) = -\nabla.(\rho \mathbf{u}\mathbf{u} + F\mathbf{B}\mathbf{B}) - \nabla(P + \tfrac{1}{2}F|\mathbf{B}|^2) + (m+1)\rho\hat{\mathbf{z}} + \nabla.\boldsymbol{\tau}, \tag{1}$$

$$\frac{\partial \mathbf{B}}{\partial t} = \nabla \times (\mathbf{u} \times \mathbf{B}) + \zeta_0 \bar{K} \nabla^2 \mathbf{B}, \qquad \nabla.\mathbf{B} = 0, \tag{2}$$

$$\frac{\partial \rho}{\partial t} = -\nabla.(\rho \mathbf{u}), \qquad P = T\rho, \tag{3}$$

$$\begin{aligned} \frac{\partial}{\partial t}\{\rho[T/(\gamma-1) + \tfrac{1}{2}|\mathbf{u}|^2 - (m+1)z] + \tfrac{1}{2}F|\mathbf{B}|^2\} \\ = -\nabla.\{\rho[\gamma T/(\gamma-1) + \tfrac{1}{2}|\mathbf{u}|^2 - (m+1)z]\mathbf{u} \\ + F\mathbf{B} \times (\mathbf{u} \times \mathbf{B} - \zeta_0 \bar{K} \nabla \times \mathbf{B} - \bar{K}\nabla T + \mathbf{u}.\boldsymbol{\tau}\}, \end{aligned} \tag{4}$$

where $\gamma = 5/3$ and the viscous stress tensor

$$\tau_{ij} = \sigma \bar{K}(\partial u_i/\partial x_j + \partial u_j/\partial x_i - \tfrac{2}{3}\delta_{ij}\partial u_k/\partial x_k) \tag{5}$$

(Hurlburt and Toomre, 1988; Hurlburt *et al.*, 1989; Weiss *et al.*, 1990). Here F is a measure of the magnetic energy density, $\bar{K}$ is the dimensionless thermal conductivity, σ is the Prandtl number, and ζ_0 is the ratio of the magnetic to the thermal diffusivity at the top of the layer. The Chandrasekhar number

$$Q = F/\sigma\zeta_0\bar{K}^2, \tag{6}$$

and the local Rayleigh number

$$R(z) = \gamma^{-1}(m+1)[1 - m(\gamma-1)]z^{2m+1}/(\sigma\bar{K}^2 z_0^{2m}), \tag{7}$$

while the local diffusivity ratio

$$\zeta(z) = \zeta_0 (z/z_0)^m. \tag{8}$$

We shall define a particular configuration by the values $R = R(\hat{z})$, $\zeta = \zeta(\hat{z})$, where $\hat{z} = z_0 + 1/2$, calculated at the middle of the layer.

The system (1)–(4) is solved subject to the boundary conditions

$$T(x, z_0, t) = z_0, \qquad T(x, z_0 + 1, t) = z_0 + 1, \tag{9}$$

$$w = \partial u/\partial z = B_x = 0 \qquad \text{at } z = z_0, z_0 + 1. \tag{10}$$

The total magnetic flux across the layer is fixed and equal to that for a uniform unit field, while the lateral boundary conditions are either chosen to be periodic, so that

$$T(0,z,t) = T(\lambda,z,t) \quad \text{etc.}, \tag{11}$$

or else correspond to reflection symmetry about sidewalls, so that

$$u = \partial w/\partial x = B_x = \partial T/\partial x = \partial \rho/\partial x = 0 \qquad \text{at } x = 0, \lambda. \tag{12}$$

The boundary conditions (11) and (12) are described as having $O(2)$ and Z_2 symmetry, respectively.

For the numerical experiments described here we adopt the parameter values used by Weiss *et al.* (1990, henceforth referred to as Paper I). First we choose a model atmosphere with $z_0 = 0.1$ and $m = 1$, so that $\chi = 11$. Then we set $\sigma = 1$ and $\zeta = 0.6$, so that $0.1 \leq \zeta \leq 1.1$, favouring oscillatory behaviour. Finally, we fix the Chandrasekhar number at $Q = 2000$, corresponding to a strong magnetic field. That leaves only two parameters to be varied, the Rayleigh number R and the aspect ratio λ. Choosing R fixes the value of $\bar{K}$, from (7), and hence that of F, from (6). Note, however, that the plasma beta at the middle of the layer,

$$\beta = 2\hat{z}^{m+1}/(Fz_0^m) = 3R/2000, \tag{13}$$

varies with the Rayleigh number. For the runs discussed here, $\beta \geq 60$ and the effects of compressibility are small.

The system (1)–(4), with boundary conditions (9), (10) and (11) or (12), possesses a static solution with $\mathbf{u} = \mathbf{0}$ and $\mathbf{B} = (0,0,1)$ for all values of R, and is symmetric with respect to reversals of the sense of motion. Linear stability theory can be used to locate primary bifurcations from this trivial solution (Cattaneo, 1984). For small values of λ, steady state (SS) convection sets in at a pitchfork bifurcation when $R = R^{(e)}$ but for λ sufficiently large there is a Hopf bifurcation at $R = R^{(o)}$, followed by a stationary (pitchfork) bifurcation at $R = R^{(e)}$ ($R^{(e)} > R^{(o)}$), as shown in Figure 2 of Paper I. The bifurcation of codimension two, where $R^{(o)} = R^{(e)}$, occurs at the critical point (λ_c, R_c) in the (λ, R)-parameter plane, where $\lambda_c = 0.683$, $R_c = 53100$.

Behaviour near the Hopf bifurcation depends on the choice of lateral boundary conditions. With the boundary conditions (12), which prohibit flow across the sidewalls, a single branch of periodic oscillatory (standing wave, or SW) solutions emerges from the Hopf bifurcation. With the less restrictive periodic boundary conditions (11), however, there is in addition a pair of (leftward and rightward) travelling wave (TW) solutions on a branch emerging from the same bifurcation. To determine whether standing waves or travelling waves are preferred it is necessary to enter the weakly nonlinear domain (cf. Hurlburt *et al.*, 1989).

Fully nonlinear solutions have to be obtained numerically. Our code uses a two-step Lax–Wendroff finite-difference scheme (Graham, 1975; Hurlburt and Toomre, 1988; Hurlburt *et al.*, 1989) on a square mesh with either 30 or 60 intervals in the vertical direction. Paper I (Figures 5–7) investigated behaviour for two values of λ, with periodic lateral boundary conditions. For $\lambda = 4/3$ there was a supercritical Hopf bifurcation giving rise to stable periodic solutions which persisted for $R > R^{(e)}$. For $\lambda = 2/3$ (just below the value of λ_c) there was a supercritical pitchfork bifurcation at $R^{(e)} = 53850$, followed by stable steady solutions (see Figure 9a of Paper I). These underwent a supercritical Hopf bifurcation at $R \approx 54300$; after this secondary bifurcation these were stable periodic oscillations which persisted up to $R = 100000$. In this paper we study the development of this oscillatory branch and show how it can be related to behaviour near the multiple bifurcation at the critical point (λ_c, R_c).

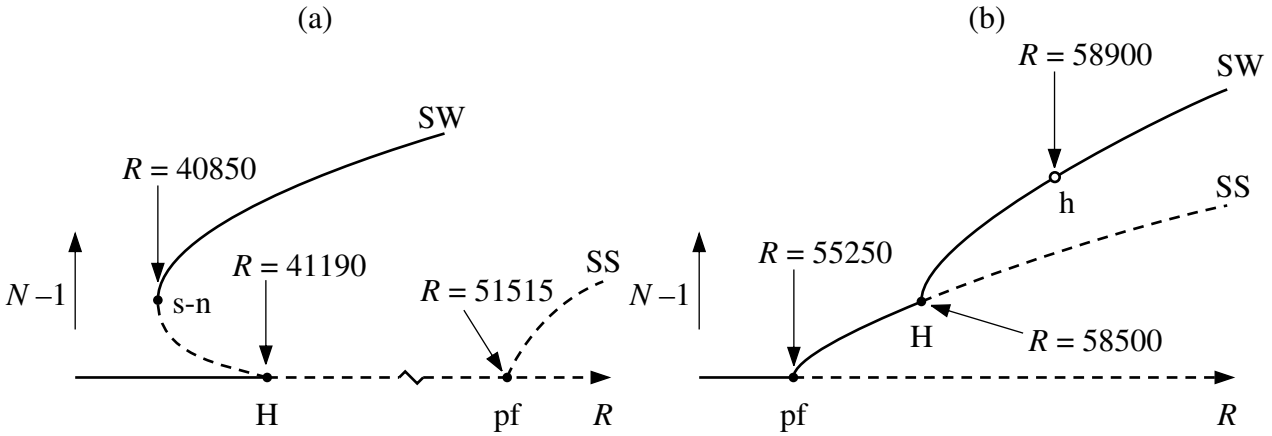

Figure 1. *Summary of numerical experiments near the critical point. (a) $\lambda = 24/30$; (b) $\lambda = 19/30$. In this and subsequent bifurcation diagrams, solid lines indicate stable (steady or oscillatory) solutions, while broken lines indicate unstable solutions. Filled circles represent Hopf (H), pitchfork (pf) or saddle-node (s-n) bifurcations; open circles represent homoclinic (h) bifurcations.*

3. NONLINEAR OSCILLATIONS

We have computed new solutions of the PDEs for values of the aspect ratio that bracket the critical value λ_c, using periodic lateral boundary conditions (11). Since all stable solutions found were either steady or standing wave solutions, results described in this section could equally well have been obtained with the no-flux boundary conditions (12). To measure the vigour of convection we evaluate the Nusselt number

$$N = \frac{F_T - \bar{K}(dT/dz)_{ad}}{\bar{K}[1 - (dT/dz)_{ad}]} = \frac{5F_T}{\bar{K}} - 4, \tag{14}$$

where F_T is the total energy flux at $z = z_0$ and $(dT/dz)_{ad} = (m+1)(\gamma-1)/\gamma = 0.8$ is the adiabatic temperature gradient. Then $(N-1)$ is a measure of the efficiency of convection, normalized with respect to the superadiabatic conductive flow.

As bifurcations are affected by discretization errors (Moore and Weiss, 1992), it is important to keep the mesh interval fixed. For behaviour near the onset of convection it suffices to use 30 intervals vertically; then the particular aspect ratios chosen are dictated by the mesh. The critical value $\lambda_c = 0.683$ corresponds to a wavenumber $\alpha_c = 2\pi/\lambda_c = 2.93\pi$. We first discuss behaviour found for $\lambda = 24/30 = 0.8$, corresponding to a wavenumber $\alpha = 2.5\pi$ and then turn to results for $\lambda = 19/30 = 0.633$ ($\alpha = 3.16\pi$), since the choice made for Paper I ($\lambda = 0.667$, $\alpha = 3\pi$) is uncomfortably close to the critical value.

Linear calculations show that when $\lambda = 0.8$ there is a Hopf bifurcation at $R^{(o)} = 41190$, followed by a pitchfork bifurcation at $R^{(e)} = 51515$. Using the nonlinear code, we have confirmed that the trivial solution is stable for $R \leq 41000$. At $R = 41000$ small perturbations (with $|N-1| \ll 0.005$) lead to periodic oscillations that decay exponentially. We have not attempted to compute nonlinear solutions in the neighbourhood of the Hopf bifurcation, but for $R = 41500$ we find that the trivial solution is unstable to growing oscillatory perturbations and there is a stable periodic solution with $1.005 \leq N \leq 1.034$. As R is increased the oscillation grows monotonically in amplitude, so that the periodic solution has $1.010 \leq N \leq 1.060$ at $R = 42000$, and has $1.082 \leq N \leq 1.450$ at $R = 50000$.

We also find subcritical oscillations. The trivial solution at $R = 41000$ has a basin of attraction that is small: large perturbations eventually settle down to low-amplitude periodic oscillations with $1.0010 \leq N \leq 1.0059$. Stable oscillations, with $1.00015 \leq N \leq 1.00096$, can also be found for $R = 40900$ but the oscillations decay for $R \leq 40800$. These results show that the Hopf bifurcation is subcritical, as indicated schematically in Figure 1(a).

Next we take $\lambda = 0.633$, when the only primary bifurcation is a supercritical pitchfork at $R^{(e)} = 55250$. At $R = 56000$ there is a stable steady solution with $N = 1.016$ and trajectories approach it monotonically. By $R = 58000$ there are decaying oscillations about a steady state with $N = 1.056$ and at $R = 58500$ the steady solution, with $N = 1.07$, is close to being unstable. At $R = 58700$ there are periodic solutions with $1.01 \leq N \leq 1.125$, corresponding to vacillation without reversal of the motion. By $R = 59000$ there are oscillations with a very long period; the flow reverses and $1.00 \leq N \leq 1.16$. By $R = 60000$ the period has dropped by 40% and the amplitude has risen so that $1.00 \leq N \leq 1.21$. This sequence is illustrated in Figure 1(b): after the pitchfork bifurcation there are two real negative eigenvalues on the stable steady branch, which merge and become complex around $R = 57000$. The real parts of the pair change sign at a supercritical Hopf bifurcation, near $R = 58500$, giving rise to a pair of vacillatory orbits about the unstable steady solutions. These orbits merge in a global gluing (or biclinic) bifurcation at $R \approx 58900$, producing an oscillation (symmetric about the origin) that grows continuously in amplitude as R is increased.

The results summarized in Figure 1 indicate what happens near the critical point. For $\lambda > \lambda_c$ there is a subcritical primary Hopf bifurcation; instead of disappearing at the codimension-two bifurcation, the Hopf bifurcation climbs up the steady branch for $\lambda < \lambda_c$. At $\lambda = \lambda_c$ the oscillatory branch swings round, so that the secondary Hopf bifurcation becomes supercritical and the whole oscillatory branch is stable. In the next section we shall see that this transition is accurately reproduced by second-order amplitude equations.

4. LOW-ORDER AMPLITUDE EQUATIONS

The behaviour we have just described is not peculiar to compressible magnetoconvection. Rather, we expect it to be generic and associated with the bifurcation of codimension two at (λ_c, R_c) in systems with Z_2 symmetry, when other parameters are appropriately chosen. The linear structure involves only two eigenvalues, which are either complex conjugates or real. Thus linear behaviour in the neighbourhood of the critical point is described by the second-order equation

$$\ddot{a} - \mu\dot{a} + \nu a = 0, \tag{15}$$

where a measures the amplitude of the motion and the stability parameters μ, ν are linearly related to R, λ. The eigenvalues, corresponding to growth-rates of perturbations to the trivial solution, are complex for $\nu > \frac{1}{4}\mu^2$ and there are two bifurcations of codimension one: a stationary bifurcation at $\nu = 0$ and a Hopf bifurcation at $\mu = 0$ for $\nu > 0$. The trivial solution is only stable for $\mu < 0$ and $\nu > 0$. When $\mu = \nu = 0$ there is a double-zero eigenvalue. This multiple bifurcation – a Takens–Bogdanov or ζ^2 (Arnéodo *et al.*, 1985) bifurcation – has been extensively studied (Arnol'd, 1983; Guckenheimer and Holmes, 1983); as we shall see, the transition point for the PDEs is indeed described by amplitude equations associated with this bifurcation.

4.1. The normal form equation

In this section we restrict our attention to solutions of the PDEs that have reflection symmetry about the lateral boundaries, so that we are only concerned with interactions between steady and standing wave solutions. Then behaviour near the codimension-two point is governed by the normal form equation for a Takens–Bogdanov bifurcation with Z_2 symmetry:

$$\ddot{a} - (\mu + ka^2)\dot{a} + (\nu + la^2)a = 0, \tag{16}$$

where k and l are real constants (Takens, 1974; Arnol'd, 1977; Knobloch and Proctor, 1981; Arnol'd, 1983; Guckenheimer and Holmes, 1983; Guckenheimer and Knobloch, 1983). This equation has the symmetry $a \to -a$ and possesses a trivial solution $a = 0$ for all μ and ν. Hence the stationary bifurcation at $\nu = 0$ is a pitchfork, giving rise to a pair of steady solutions with $a = \pm(-\nu/l)^{1/2}$ for $\nu l < 0$.

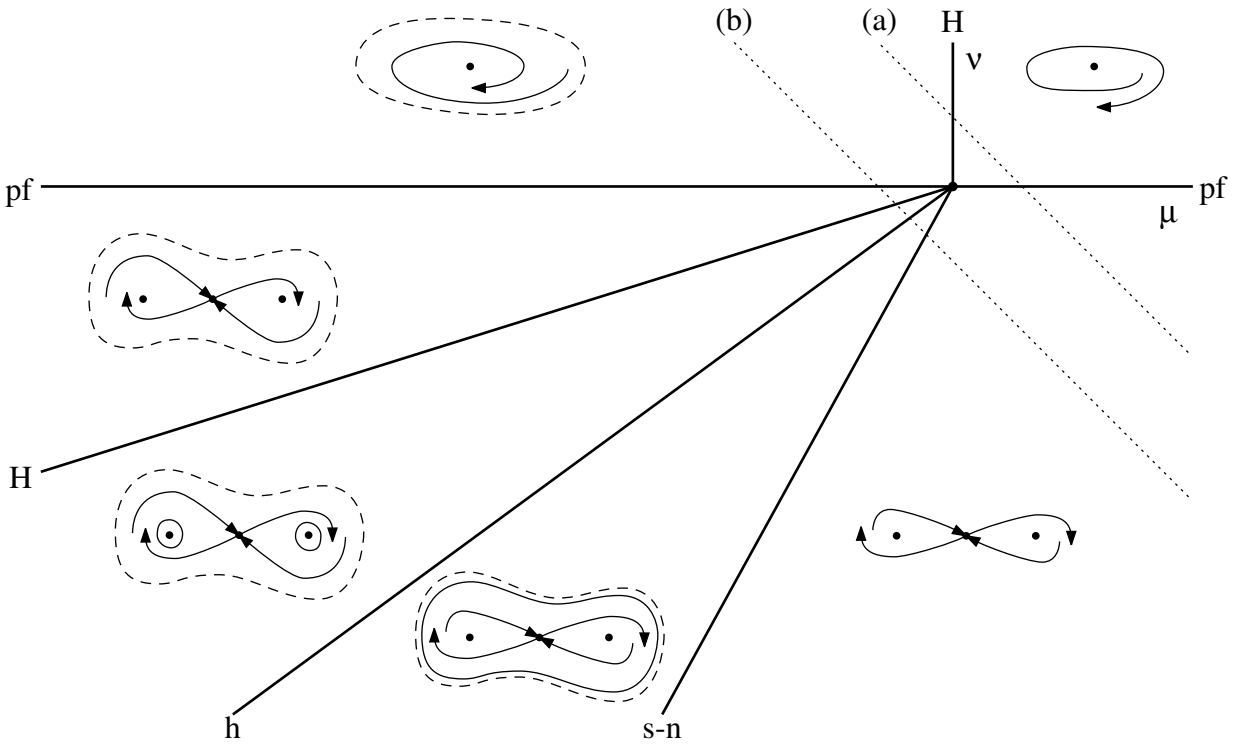

Figure 2. *Bifurcation set of equation (17) (after Arnol'd 1983). The solid lines indicate the parameter values where the behaviour of the equation undergoes a qualitative change. Phase portraits in the $(a, \dot{a})$-plane are sketched in the regions in between the bifurcation lines: stable and unstable periodic orbits are represented as solid and dashed lines respectively. Bifurcation diagrams along the two slices (a) and (b) are shown in Figure 3.*

The case $l < 0$ describes subcritical steady convection and is relevant to thermosolutal convection (e.g. Coullet and Spiegel, 1983; Proctor and Weiss, 1990) and to magnetoconvection when λ is large (Proctor and Weiss, 1982). We are interested in the case $l > 0$, with supercritical steady convection, which applies to magnetoconvection when λ is sufficiently small (Knobloch and Proctor, 1981). The sign of k determines whether the Hopf bifurcation is supercritical or subcritical. Since we are interested in a subcritical Hopf bifurcation, we take $k > 0$. By rescaling a and t we may (without loss of generality) set $k = l = 1$, so that (16) reduces to

$$\ddot{a} - (\mu + a^2)\dot{a} + (\nu + a^2)a = 0. \tag{17}$$

Note that by reversing the direction of time and changing the sign of μ we can transform (17) into (16) with $k = -1$, $l = 1$ (Arnol'd, 1983). This is a standard case, whose properties are well understood. From the unfolding diagrams given, for example, by Arnol'd (1983, Figure 143), Guckenheimer and Holmes (1983, Figure 7.3.9) or Guckenheimer and Knobloch (1983, Figure 1) we can easily construct the corresponding diagram for equation (17). Figure 2 shows the bifurcation set in the (μ, ν)-plane, together with sketched phase portraits in the $(a, \dot{a})$-plane. With $\nu > 0$ and $\mu < 0$, the stable trivial solution is circled by an unstable periodic orbit. The nontrivial steady solutions, with $a^2 = -\nu$, exist only for $\nu < 0$. The lines in the third quadrant indicate, first, the pitchfork bifurcation ($\nu = 0$), then a secondary Hopf bifurcation from the nontrivial steady solution at $\nu = \mu$ ($\mu < 0$) (in which stable vacillatory orbits are created when a pair of complex eigenvalues cross the real axis), followed by a global gluing bifurcation, where there is a pair of homoclinic connections at $\nu = \frac{5}{4}\mu$ ($-1 \ll \mu < 0$). Finally, there is a saddle-node bifurcation of the periodic orbit.

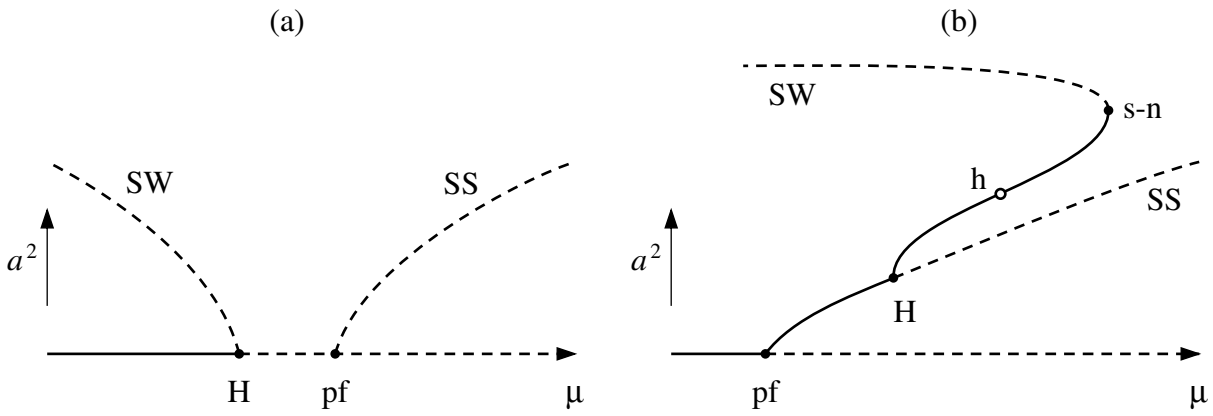

Figure 3. *Bifurcation diagrams along the two slices in Figure 2: a^2 as a function of μ. (a) $\mu+\nu>0$; (b) $\mu+\nu<0$.*

In order to appreciate the significance of this bifurcation diagram we need to consider the codimension-one behaviour that would result from decreasing ν and increasing μ along the two lines marked in Figure 2 (which correspond to increasing R for fixed λ in the PDEs). This behaviour is represented by the bifurcation diagrams in Figure 3, which show a^2 as a function of μ. The first diagram, in Figure 3(a), shows a subcritical Hopf bifurcation, followed by a (subcritical) pitchfork bifurcation; both the oscillatory and the steady branch are unstable. In Figure 3(b) there is a supercritical pitchfork bifurcation, leading to stable solutions on the steady branch. Near the primary bifurcation there are two real negative eigenvalues that merge, giving a complex pair whose real part changes sign when $\mu=\nu$. The supercritical Hopf bifurcation gives rise to stable periodic solutions, or orbits, that enclose the two unstable foci at $a=\pm|\nu|^{1/2}$. These vacillatory orbits merge in the gluing bifurcation to give a single stable oscillation of period P, which is symmetric about the origin in the $(a,\dot{a})$-phase plane, so that $a(t+\frac{1}{2}P)=-a(t)$. Subsequently, the oscillations lose stability in a saddle-node bifurcation.

It is only when k and l are both positive in (16) that the Hopf bifurcation climbs up the steady branch after the multiple bifurcation, as in Figure 3(b). For all other choices of k and l, only the branch of steady solutions would be present when $\mu+\nu<0$. Although the bifurcation diagrams in Figure 3 can be recognized within the more elaborate structures catalogued by Dangelmayr and Knobloch (1987, cases I+ (a) and (b), II+ (a) and (b) of Figure 8) their significance had not hitherto been appreciated. What we have shown is that, if the steady branch is supercritical ($l>0$) and the Hopf bifurcation is subcritical ($k>0$) just before the codimension-two bifurcation, then there is a branch of stable periodic orbits emerging from a secondary Hopf bifurcation, whose existence could not be predicted from the linear equation (15).

4.2. Effects of adding fifth-order terms

The normal form equation (17) provides a qualitatively accurate description of behaviour in a small (but finite) neighbourhood of the origin in the parameter plane i.e., for $\mu^2, \nu^2 \ll 1$. Thus it cannot represent the saddle-node bifurcation in Figure 1(a), through which the oscillatory branch acquires stability. There is a systematic procedure which allows one to go further: the coefficients k and l of the cubic terms in (16) may be regarded as small parameters so that, in order to treat behaviour near the codimension-four bifurcation where $\mu = \nu = k = l = 0$, it is necessary to add fifth-order terms to the equation (cf. Dangelmayr, Armbruster and Neveling, 1985). This introduces an unwelcome plethora of different cases, so we shall follow an alternative approach and simply add appropriate fifth-order terms. Then the normal form equation (17) becomes

$$\ddot{a} - (\mu + a^2 - ma^4)\dot{a} + (\nu + a^2 + na^4)a = 0. \tag{18}$$

The case with $m = 0$, $n \neq 0$, which does not include a saddle-node bifurcation on the subcritical oscillatory branch, has already been analysed in detail (Dangelmayr *et al.*, 1985; Knobloch and Proctor 1988). We require $m > 0$, $n \geq 0$ so as to allow the oscillatory branch in Figure 3(a) to turn round without significantly affecting the steady branch. This case, with $n = 0$, has been studied independently by Rodríguez-Luis, Freire and Ponce (1991). Although a nonlinear transformation relates the cases ($m = 0$, $n \neq 0$), ($m \neq 0$, $n = 0$) and ($m \neq 0$, $n \neq 0$), the qualitative behaviour of the nonlinear solutions may be different outside the immediate neighbourhood of $(\mu, \nu) = (0, 0)$.

We have investigated the case $m = 1$, $n = 1$ numerically, using the AUTO continuation package (Doedel, 1986). The bifurcation set is shown in Figure 4(a). In the region near the origin, which is enlarged in Figure 4(b), the pattern follows the unfolding of the codimension-two bifurcation in Figure 2 but non-local behaviour is quite different. A line of saddle-node bifurcations enters from the quadrant with $\mu < 0$, $\nu > 0$ and meets the original line in a cusp. The lines of Hopf and gluing bifurcations turn round for μ sufficiently negative and eventually cross into the quadrant with $\mu > 0$. When the line of gluing bifurcations crosses into the region where $\mu > 0$, which is enlarged in Figure 4(c), the eigenvalues of the trivial solution change order, such that the positive one becomes larger in magnitude than the negative one. It is these eigenvalues that determine the stability of the periodic orbits involved in the gluing bifurcation: as periodic orbits approach the gluing bifurcation, their periods go to infinity since the system spends more and more of its time near the trivial solution. Here, the dynamics is dominated by the linear part of the flow (Guckenheimer and Holmes, 1983). If the negative eigenvalue is larger in magnitude than the positive eigenvalue (as it is when $\mu < 0$), then the periodic orbit approaching the homoclinic bifurcation must be stable: contraction is stronger than expansion. Conversely, if the negative eigenvalue is smaller in magnitude than the positive eigenvalue (as it is when $\mu > 0$), then the periodic orbit approaching the homoclinic bifurcation must be unstable. Thus as the line of gluing bifurcations crosses from $\mu < 0$ to $\mu > 0$ the stability of the periodic orbits involved in the gluing bifurcation has to change at $\mu = 0$. This change is associated with the appearance of a pair of lines of saddle-node bifurcations, which are created in a cusp at $\mu = 0$ (Rodríguez-Luis *et al.*, 1991). One of the two lines of saddle-node bifurcations connects to the line of Hopf bifurcations at a point where the Hopf bifurcation changes from being supercritical to subcritical. This connection cannot occur unless we have m and n both non-zero. The solutions are profoundly affected by these changes; to illustrate them, we construct bifurcation diagrams in Figure 5 corresponding to the arbitrarily chosen lines marked in the (μ, ν)-plane in Figure 4(a).

In Figure 5(a), corresponding to a line that avoids the third quadrant, the subcritical Hopf bifurcation is preceded by a saddle-node bifurcation, giving rise to stable periodic solutions. This matches the behaviour found for the PDEs in Figure 1(a). Moreover, the oscillatory branch eventually rejoins the steady branch in a subcritical Hopf bifurcation, following a saddle-node bifurcation and a gluing bifurcation. The steady solutions thus acquire stability. Behaviour immediately after the codimension-two bifurcation is represented in Figure 5(b): the secondary Hopf bifurcation is

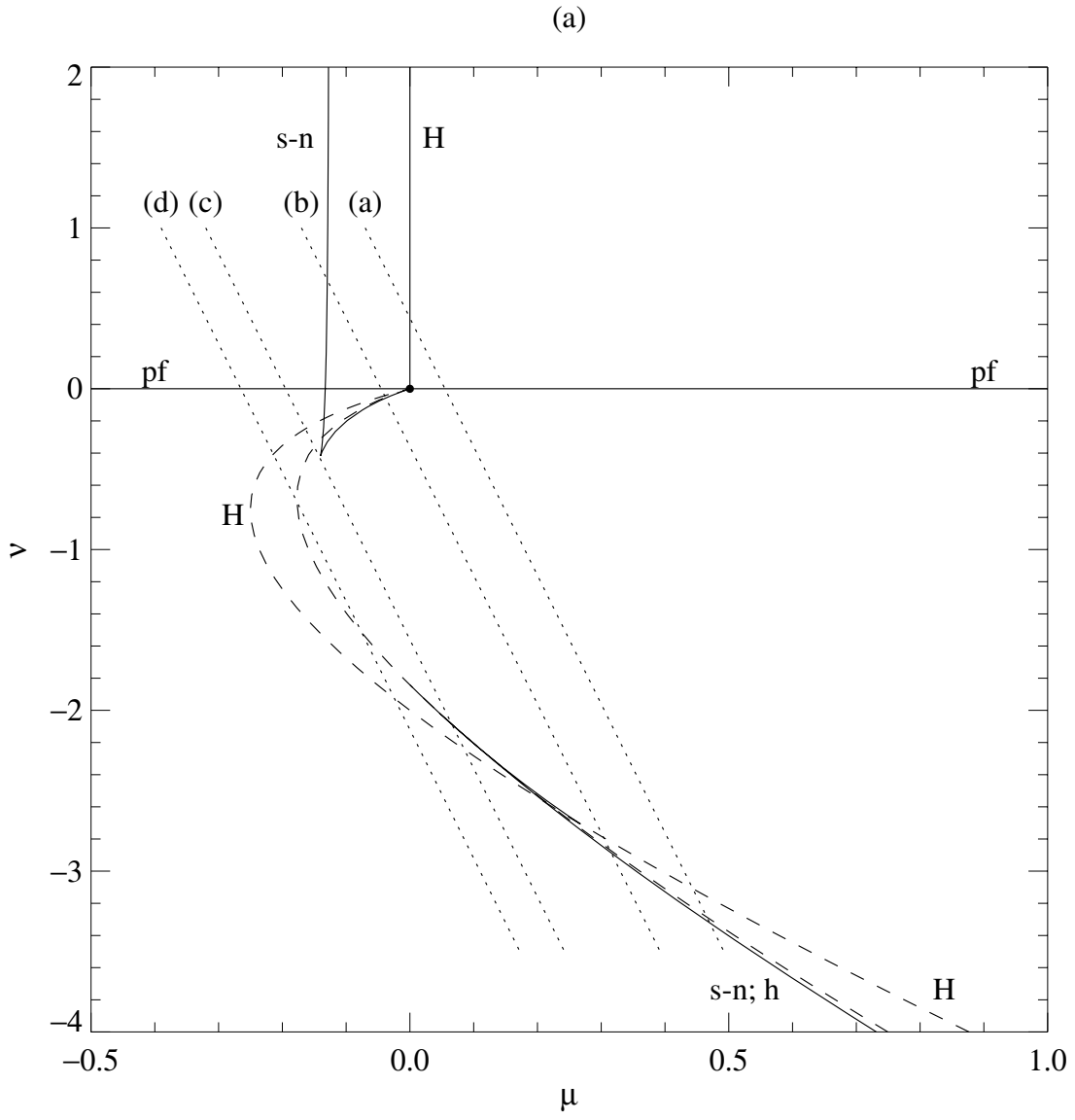

Figure 4. *(a) Numerically computed bifurcation set of equation (18) with* $m = 1$ *and* $n = 1$*. Bifurcation diagrams along the dotted lines labelled (a)–(d) are shown in Figure 5. For clarity, the line of Hopf bifurcations from the steady solutions and the line of gluing bifurcations are shown as dashed lines. These lines cross near* $(\mu, \nu) = (0.22, -2.6)$.

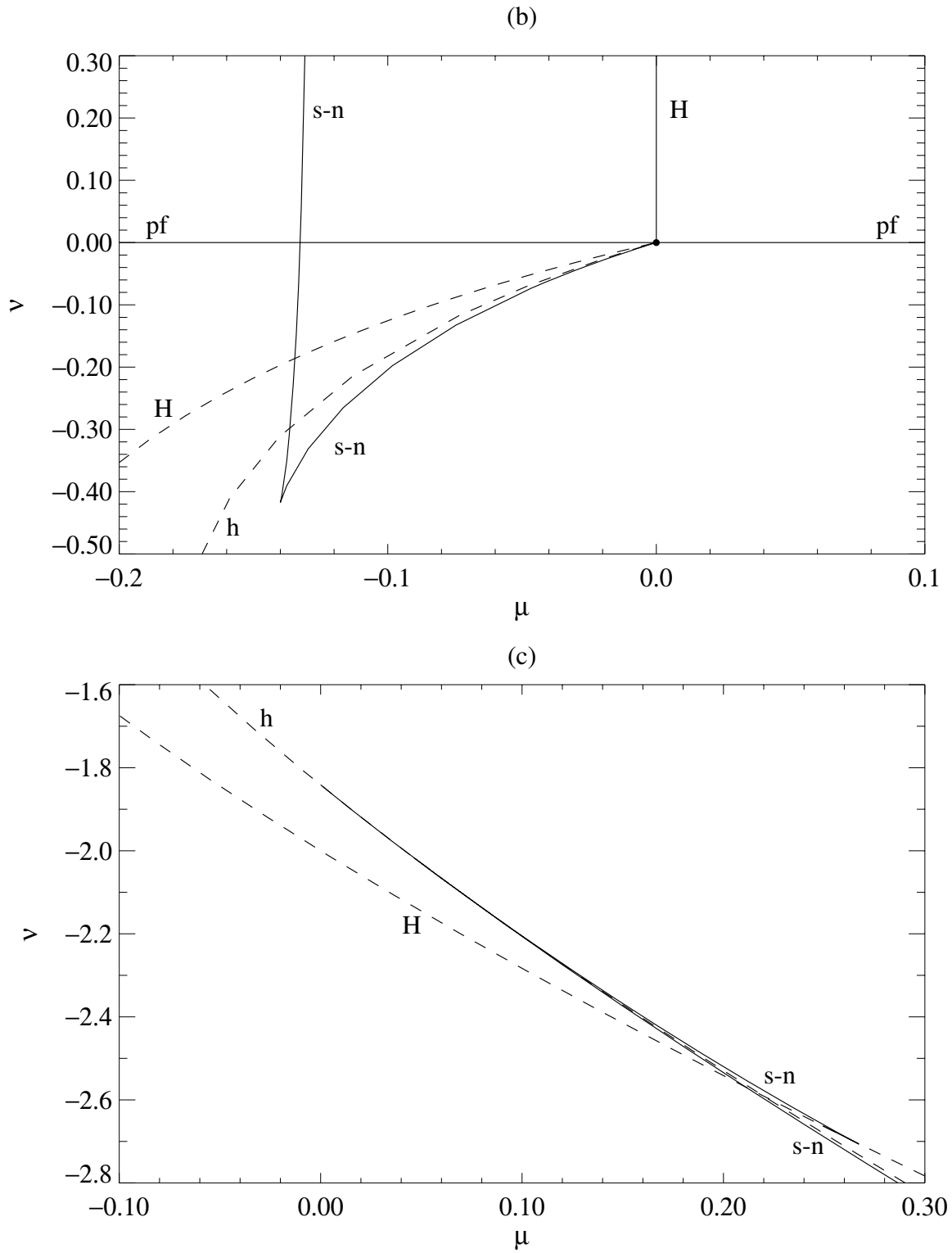

Figure 4 (continued). *(b) Detail of the bifurcation set of equation (18), near the critical point. Compare with Figure 2. (c) Detail where the line of gluing bifurcations crosses into the $\mu > 0$ half-plane.*

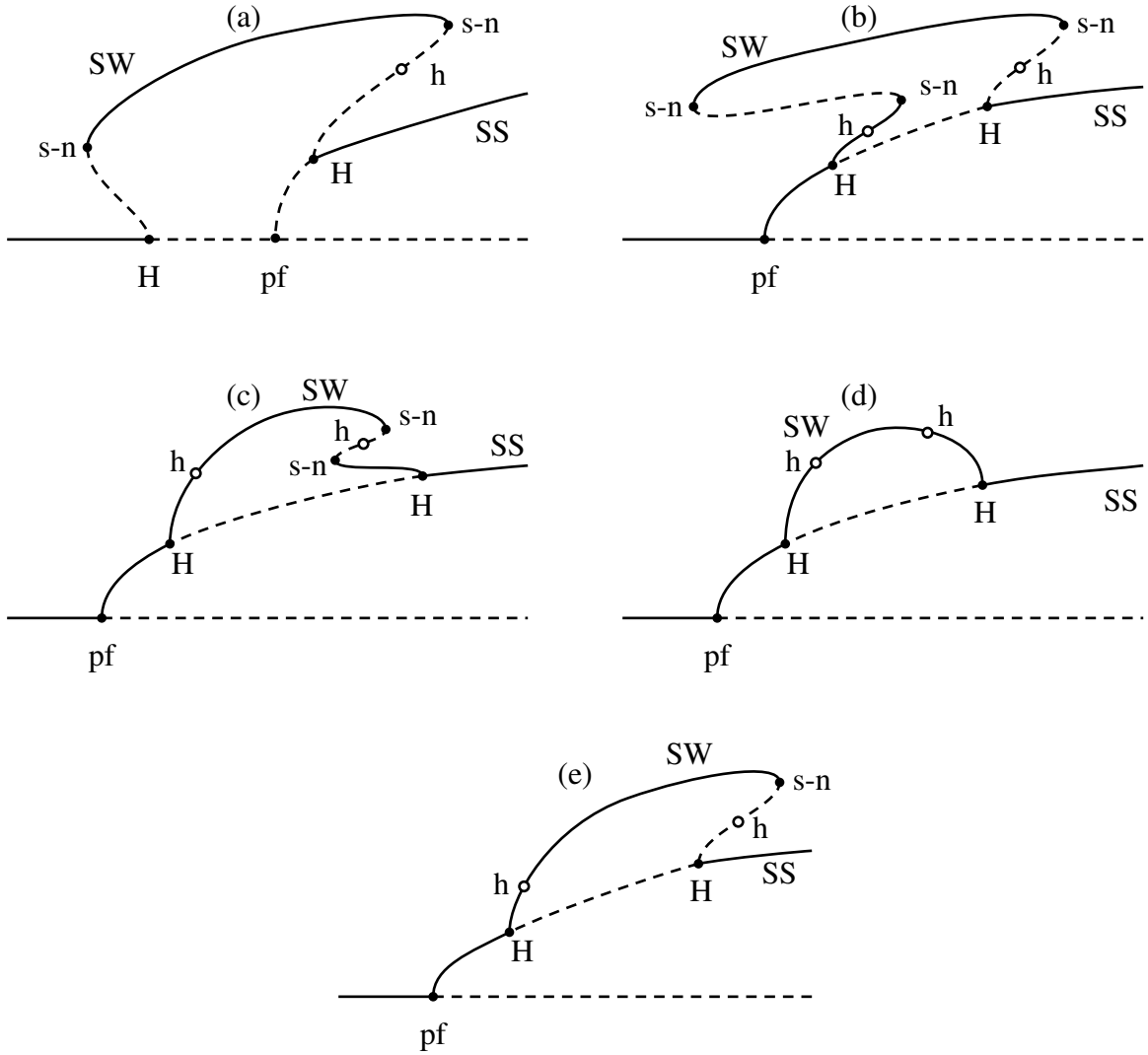

Figure 5. *Bifurcation diagrams for equation (18): (a)–(d) along the four slices marked in Figure 4(a); (e) is a combination of the left halves of (c)–(d) and the right halves of (a)–(b), corresponding to a less-steep slice through Figure 4(a).*

supercritical and is followed, as in Figure 3(b), by a gluing bifurcation and a saddle-node bifurcation. But now there is a second turning point on the oscillatory branch, which gains stability at a saddle-node bifurcation that actually precedes the pitchfork bifurcation. Hence there are stable periodic oscillations over a range extending from the initial to the final saddle-node bifurcations.

As the line in Figure 4 is shifted away from the multiple bifurcation the initial saddle-node bifurcation moves across the bifurcation diagram, passing first the pitchfork bifurcation, then the gluing bifurcation, and finally disappearing in a cusp singularity with the saddle-node bifurcation that follows the gluing bifurcation (Figure 5(c)). Next, the other pair of saddle-node bifurcations disappears in another cusp singularity. Eventually, there is only a single branch of stable periodic orbits, linking two supercritical Hopf bifurcations, with two gluing bifurcations, as shown in Figure 5(d). This bifurcation diagram is consistent with the behaviour found in numerical experiments and shown in Figure 1(b). Shifting the line yet further away causes the two Hopf bifurcations to approach until they eventually disappear, leaving only a stable steady branch.

It can be shown that the final Hopf bifurcation is always supercritical when $n = 0$. The only qualitative effect of the term proportional to a^5 ($n > 0$) is to allow the final Hopf bifurcation to become subcritical for ν sufficiently negative and μ positive. This allows, for instance, a bifurcation diagram with the appearance sketched in Figure 5(e): the oscillatory branch loses stability in a saddle-node bifurcation. In the bifurcation diagram, the gluing bifurcation lies on the unstable portion of the oscillatory branch, between the turning point and the subcritical tertiary Hopf bifurcation.

5. THE TERTIARY HOPF BIFURCATION: STANDING WAVES AND TRAVELLING WAVES

In each of the bifurcation diagrams of Figure 5 the oscillatory branch ends in a Hopf bifurcation on the steady branch, which retains stability thereafter. We now return to the PDEs in order to investigate this final transition. Since it is non-local, occurring far from the primary bifurcations, we do not expect details to be sensitive to the choice of λ. So we shall investigate a single value, $\lambda = 2/3$, for which the oscillatory branch appears at a secondary Hopf bifurcation (cf. Section 2). The mesh has 60 intervals vertically, and discretization errors do not significantly affect the bifurcation structure. Although the same solutions remain stable near the primary and secondary bifurcations for either choice of lateral boundary conditions, behaviour near the tertiary bifurcation does depend on whether periodic or mirror-symmetric boundary conditions are adopted. We begin therefore by imposing the no-flux boundary conditions (12), so that the numerical experiments are consistent with the amplitude equations presented in the previous section.

5.1. A subcritical Hopf bifurcation

For R sufficiently large, the steady branch is stable. At $R = 150000$, for example, there is a steady solution with $N = 3.6$. With the boundary conditions (12) the steady branch can be followed down to $R = 100000$, where $N = 1.85$. At $R \approx 99000$ the steady branch becomes unstable to growing oscillations, which develop into a stable periodic solution, with reversals of the flow and $1.2 \leq N \leq 3.4$. The oscillatory branch continues up to $R \approx 107500$, where it loses stability in a saddle-node bifurcation. The bifurcation structure found in these numerical experiments is illustrated in Figure 6(a). The oscillatory branch apparently ends in a subcritical tertiary Hopf bifurcation and the overall pattern is similar to that in Figure 5(e).

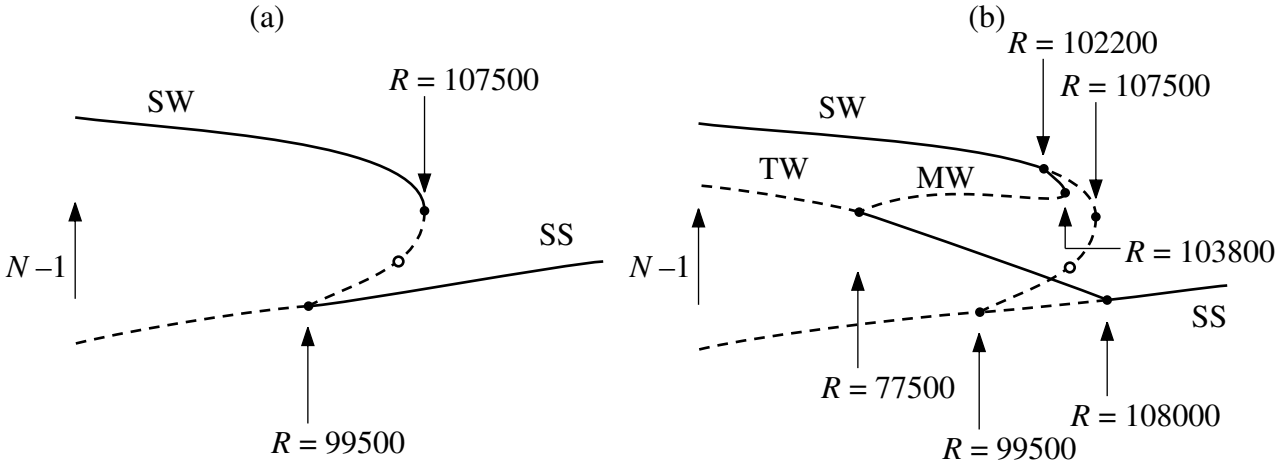

Figure 6. *Summary of numerical experiments with $\lambda = 2/3$. (a) With Z_2 (reflecting) boundary conditions (12); (b) with $O(2)$ (periodic) boundary conditions (11).*

5.2. Travelling wave solutions

Next we impose the less restrictive periodic boundary conditions (11), which allow both standing wave and travelling wave solutions. Now we find that the steady branch is stable for $150000 \geq R \geq 110000$ but undergoes a pitchfork bifurcation at $R = R_t \approx 108000$, giving rise to a pair of left- and rightward travelling waves. As R is decreased the phase velocity of the waves increases, locally as $(R_t - R)^{1/2}$, while the Nusselt number gradually falls. The branch of travelling wave solutions remains stable down to $R = 78000$, where $N = 1.60$. At $R = 77000$ the travelling waves are unstable to oscillatory perturbations, which develop into a standing wave solution with $1.15 \leq N \leq 2.12$. The standing waves remain stable as R is increased up to $R = 102000$. At $R = 104000$, trajectories are attracted to the travelling wave solution.

This hysteresis requires the existence of an intermediate branch of modulated waves that connects the branches of standing wave and travelling wave solutions. We indeed find such a branch of stable modulated wave solutions, which leaves the standing wave branch in a supercritical pitchfork bifurcation at $R \approx 102200$. Solutions on this branch are spatially asymmetric and drift very slowly as they oscillate. The maximum value of N is 3–5% lower than that for the unstable standing wave solutions. Apparently the modulated waves lose stability in a saddle-node bifurcation at $R \approx 103800$. We presume that the branch of unstable modulated waves eventually meets the travelling wave branch in a subcritical Hopf bifurcation at $R \approx 77500$, as depicted in Figure 6(b). This bifurcation structure is consistent with the results already obtained in Figure 6(a) and with transitions between standing waves and travelling waves in other problems (cf. Hurlburt *et al.*, 1989). It can also be related to appropriate low-order amplitude equations.

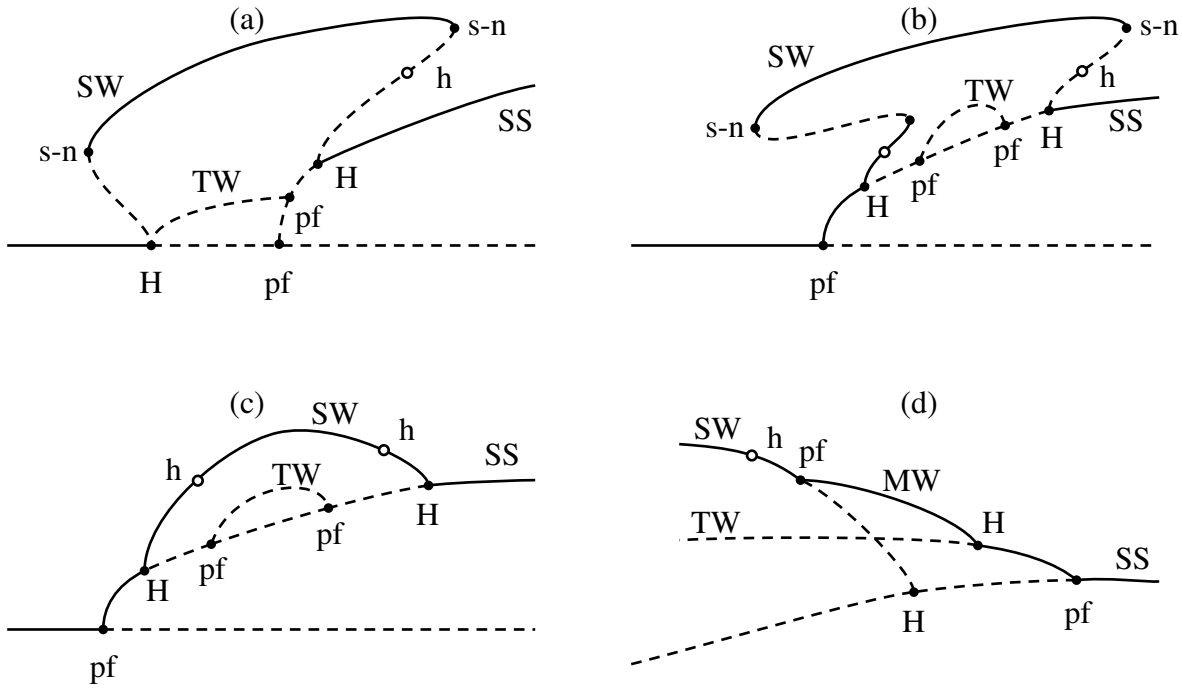

Figure 7. *Schematic bifurcation diagrams with travelling waves. (a)–(c) correspond to Figure 5(a), (b) and (d): the travelling wave branch is always unstable. In (d), the Hopf and pitchfork bifurcations on the steady branch have crossed, and stability is transferred from standing waves to travelling waves via an intermediate branch of modulated waves.*

6. AMPLITUDE EQUATIONS FOR TRAVELLING WAVES

Branches of travelling and standing waves emerge together from the primary bifurcation for $\lambda > \lambda_c$. Their behaviour is described by the fourth-order normal form equations for a Takens–Bogdanov bifurcation with $O(2)$ symmetry, which have been thoroughly investigated by Dangelmayr and Knobloch (1987). If we assume that the travelling waves bifurcate supercritically, the bifurcation diagrams in Figure 3(a) and (b) are modified as shown in Dangelmayr and Knobloch (1987, Figure 8, cases I+ (b) and I+ (a)). The only addition to Figure 3(a) would be an unstable branch of travelling wave solutions. After the codimension-two bifurcation both standing waves and travelling waves bifurcate separately from the subcritical steady branch and the Hopf bifurcation precedes the pitchfork. This behaviour is included in Figures 7(a) and (b).

The normal form equations can be modified by adding higher order terms and it is easy to predict how bifurcation diagrams might be altered. Among the many possibilities is the obvious sequence in Figure 7(a), (b) and (c), which correspond to the cases in Figure 5(a), (b) and (d). In these diagrams the travelling waves are always unstable. Inclusion of modulated waves allows more complicated behaviour. In Figure 7(c) there is a tertiary Hopf bifurcation from the steady branch, which is followed by a pitchfork bifurcation, giving rise to travelling waves, as the parameter μ is decreased. If these two bifurcations cross we expect that stability will be transferred from travelling waves to standing waves via an intermediate branch of modulated waves, as depicted in Figure 7(d). By distorting this pattern, we can recover the bifurcation structure actually found for the PDEs and illustrated in Figure 6(b).

7. CONCLUSION

In this paper we have used a specific model problem to illuminate a general property of nonlinear convection. We have shown how, even when linear theory yields only monotonically growing instability, oscillatory solutions may appear at a secondary Hopf bifurcation, and confirmed that this behaviour is associated with a multiple bifurcation of codimension two that is preceded by a subcritical Hopf bifurcation. Moreover, the secondary Hopf bifurcation is described by the familiar Takens–Bogdanov normal form equations – once they are appropriately reinterpreted. To complete the picture it is necessary to extend these amplitude equations by adding higher order terms. The resulting system describes all the qualitative features found in our numerical experiments, including not only periodic solutions (standing waves) but also travelling waves. The PDEs that we have solved happen to be those governing two-dimensional compressible convection but we expect similar behaviour to appear in two- or three-dimensional Boussinesq magnetoconvection, or in the presence of rotation, or indeed in any system where there is a Takens–Bogdanov bifurcation with suitably chosen parameters.

This treatment shows how apparently complicated behaviour in numerical experiments can be interpreted, after a systematic investigation, by relating the PDEs to appropriate low-order systems of ODEs (the amplitude equations) that can then be solved with much greater precision. Our particular example demonstrates how this process can be successfully carried out for two-dimensional rolls with a fixed aspect ratio. The same approach can be used to study bifurcations involving changes in spatial symmetry as well as in temporal properties: the real challenge now is to analyse the much richer spatiotemporal behaviour in three-dimensional convection.

Acknowledgements

This project grew out of a collaboration with Neal Hurlburt and has benefited from discussions with Vladimir Arnol'd. The work was supported by the Science and Engineering Research Council, while AMR held a Commonwealth Scholarship.

Arnéodo, A., Coullet, P.H., Spiegel, E.A. and Tresser, C., "Asymptotic chaos," *Physica* **14D**, 327–347 (1985).

Arnol'd, V.I., "Loss of stability of self-oscillations close to resonance and versal deformations of equivariant vector fields," (in Russian) *Funct. Anal. Applic.* **11**, 1–10 (1977).

Arnol'd, V.I., *Geometrical Methods in the Theory of Ordinary Differential Equations*, Springer, New York (1983).

Cattaneo, F., "Oscillatory convection in sunspots," in: *The Hydromagnetics of the Sun* (eds. Guyenne, T.D. and Hunt, J.J.) pp. 47–50, ESA SP-220, Noordwijkerhout (1984).

9479–524

Coullet, P.H. and Spiegel, E.A., "Amplitude equations for systems with competing instabilities," *SIAM J. Appl. Math.* **43**, 776–821 (1983).

Dangelmayr, G., Armbruster, D. and Neveling, M., "A codimension three bifurcation for the laser with saturable absorber," *Z. Phys. B – Condensed Matter* **59**, 365–370 (1985).

Dangelmayr, G. and Knobloch, E., "The Takens–Bogdanov bifurcation with $O(2)$-symmetry," *Phil. Trans. R. Soc. Lond. A* **A322**, 243–279 (1987).

Doedel, E. and Kernévez, J., *AUTO: Software for Continuation and Bifurcation Problems in Ordinary Differential Equations*, CalTech Press, Pasadena (1986).

Graham, E., "Numerical simulation of two-dimensional compressible convection," *J. Fluid Mech.* **70**, 689–703 (1975).

Guckenheimer, J. and Knobloch, E., "Nonlinear convection in a rotating layer: amplitude expansions and normal forms," *Geophys. Astrophys. Fluid Dynamics* **23**, 247–272 (1983).

Guckenheimer, J. and Holmes, P., *Nonlinear Oscillations, Dynamical Systems and Bifurcations of Vector Fields*, Springer, New York (1983).

Hughes, D.W. and Proctor, M.R.E., "Magnetic fields in the solar convection zone: magnetoconvection and magnetic buoyancy," *Annu. Rev. Fluid Mech.* **20**, 187–223 (1988).

Hurlburt, N.E. and Toomre, J., "Magnetic fields interacting with nonlinear compressible convection," *Astrophys. J.* **327**, 920–932 (1988).

Hurlburt, N.E., Proctor, M.R.E., Weiss, N.O. and Brownjohn, D.P., "Nonlinear compressible magnetoconvection. Part 1. Travelling waves and oscillations," *J. Fluid Mech.* **207**, 587–628 (1989).

Knobloch, E. and Proctor, M.R.E., "Nonlinear periodic convection in double-diffusive systems," *J. Fluid Mech.* **108**, 291–316 (1981).

Knobloch, E. and Proctor, M.R.E., "The double Hopf bifurcation with 2 : 1 resonance," *Proc. R. Soc. Lond.* A **415**, 61–90 (1988).

Moore, D.R. and Weiss, N.O., "Sensitivity of bifurcations to discretization," in: *Dynamics of Numerics and Numerics of Dynamics* (eds. Broomhead, D.S. and Iserles, A.) pp. 107–125, Clarendon Press, Oxford (1992).

Proctor, M.R.E., "Magnetoconvection," in: *Sunspots: Theory and Observations* (eds. Thomas, J.H. and Weiss, N.O.) pp. 221–241, Kluwer, Dordrecht (1992).

Proctor, M.R.E. and Weiss, N.O., "Magnetoconvection," *Rep. Prog. Phys.* **45**, 1317–1379 (1982).

Proctor, M.R.E. and Weiss, N.O., "Normal forms and chaos in thermosolutal convection," *Nonlinearity* **3**, 619–637 (1990).

Rodríguez-Luis, A.J., Freire, E. and Ponce, E., "On a codimension 3 bifurcation arising in an autonomous electronic circuit," *International Series of Numerical Mathematics* **97**, 301–306 (1991).

Takens, F., "Forced oscillations and bifurcations," *Comm. Math. Inst., Rijksuniversiteit Utrecht* **3**, 1–59 (1974).

Weiss, N.O., "Magnetoconvection," *Geophys. Astrophys. Fluid Dynamics* **62**, 229–247 (1991).

Weiss, N.O., Brownjohn, D.P., Hurlburt, N.E. and Proctor, M.R.E., "Oscillatory convection in sunspot umbrae," *Mon. Not. R. Astron. Soc.* **245**, 434–452 (1990).

OSCILLATIONS AND SECONDARY BIFURCATIONS IN NONLINEAR MAGNETOCONVECTION

A.M. RUCKLIDGE, N.O. WEISS, D.P. BROWNJOHN and M.R.E. PROCTOR

Department of Applied Mathematics and Theoretical Physics,
University of Cambridge, Cambridge CB3 9EW, UK

Abstract

Complicated bifurcation structures that appear in nonlinear systems governed by partial differential equations (PDEs) can be explained by studying appropriate low-order amplitude equations. We demonstrate the power of this approach by considering compressible magnetoconvection. Numerical experiments reveal a transition from a regime with a subcritical Hopf bifurcation from the static solution to one where finite-amplitude oscillations persist although there is no Hopf bifurcation from the static solution. This transition is associated with a codimension-two bifurcation with a pair of zero eigenvalues. We show that the bifurcation pattern found for the PDEs is indeed predicted by the second-order normal form equation (with cubic nonlinearities) for a Takens–Bogdanov bifurcation with Z_2 symmetry. We then extend this equation by adding quintic nonlinearities and analyse the resulting system. Its predictions provide a qualitatively accurate description of solutions of the full PDEs over a wider range of parameter values. Replacing the reflecting (Z_2) lateral boundary conditions with periodic ($O(2)$) boundaries allows stable travelling wave and modulated wave solutions to appear; they could be described by a third-order system.

Keywords: Magnetoconvection, bifurcation theory, amplitude equations, Takens–Bogdanov bifurcation, gluing bifurcation

Submitted to *Geophysical and Astrophysical Fluid Dynamics*, December, 1991; revised June, 1992.

Geophys. Astrophys. Fluid Dynamics **68** 133–150 (1993).